

Energy Loss and Straggling of Alpha Particles in Metal Foils*

J. R. COMFORT, J. F. DECKER, E. T. LYNK, M. O. SCULLY, AND A. R. QUINTON†

Physics Department, Yale University, New Haven, Connecticut

(Received 12 April 1966)

The energy loss and energy straggling of charged particles in foils of aluminum, nickel, silver, and gold have been studied as a function of total material thickness and of particle energy using 8.78 MeV Th C' alpha particles and solid-state detectors. Energy thickness, stopping power, and straggling curves were obtained. The straggling results are compared with theoretical predictions of Bohr, Bethe, and Livingston, and of Titeica. Large discrepancies are found at low energy. Foil inhomogeneities and multiple scattering will probably not account fully for these. It is suggested that the effects of capture and loss of electrons, and the fluctuations of charge exchange are primarily responsible.

I. INTRODUCTION

ALTHOUGH the penetration of charged particles in matter has long been studied and reviewed¹⁻⁵ extensively, an aspect of this subject frequently considered only briefly is the statistical fluctuation occurring in the energy-loss processes resulting in an energy broadening of an initially monoenergetic beam of particles. This phenomenon, called straggling, is measured by the root-mean-square (rms) deviation of the energy distribution about its mean value. It is often of importance to experimental nuclear physicists. For example, the understanding of the observed thick-target yields near (p, γ) resonances requires an exact knowledge of the energy distribution of the particles in the targets.⁶ The resolution capability of nuclear reactions is frequently limited by the target thickness, and knowledge of the limitations is often desired.

Although the theoretical understanding of both energy loss and straggling is well advanced, experimental information is generally limited. Measurements have often been made at particle velocities greater than those of the atomic electrons in the material, corresponding to about 1-MeV equivalent proton energy, and good agreement with theory has been obtained. Difficulties, however, have occasionally been reported at low energies where the capture and loss of electrons and the failure of all but the outermost electrons to participate in the stopping processes have not been completely or successfully incorporated into the theory. Early stopping power ($-dE/dx$) and straggling measurements^{7,8} of low-energy protons showed some discrepancies with theory. More recent measure-

ments of energy loss and straggling of 1.5- to 4.5-MeV protons and deuterons in various metals⁹ have been successfully understood.¹⁰ But measurements of energy straggling of 5-MeV alpha particles have shown large disagreement with theory for aluminum and some discrepancy for mica.^{11,12}

This report will discuss measurements made of the stopping power and straggling of natural alpha particles in passing through thin foils of aluminum, nickel, silver, and gold. The foils were added successively in the particle beam so that the stopping powers may be measured as a function of energy and the straggling may be measured as a function of both particle energy and total material thickness. A solid-state detector was used to achieve good energy resolution. The results obtained will be compared with those predicted by theoretical formulas.

II. THE EXPERIMENT

A. The Target Foils

Foils of the elements which were studied were commercially prepared. Those of Al and Ni were approximately 1-2 mg/cm² thick and those of Ag and Au were about 2-5 mg/cm² thick. In addition, very thick foils of Al and Ni, each approximately 4 mg/cm² thick, were used. Punched disks of measured diameter were weighed to the nearest 0.01 mg on a microbalance. Thicknesses obtained are believed to be known within 1%.

The above method supplied only the average thickness of each foil. No information is given concerning microscopic inhomogeneities. This information is vital for any experiment in which energy or range straggling is to be measured, because such irregularities can greatly enhance the measured energy or range distributions. Unfortunately, a good technique for measuring irregularities in thickness over areas less than 0.1 mm² with high precision was not available. A gross measure of the uniformity can be made by holding the foils in front of a strong light source. In this way it was found

⁹ L. P. Nielsen, Kgl. Danske Videnskab. Selskab, Mat. Fys. Medd. 33, No. 6 (1961).

¹⁰ H. Bichsel, Natl. Acad. Sci.—Natl. Res. Council Publ. 1133 (1964).

¹¹ F. Demicheli, Nuovo Cimento 13, 562 (1959).

¹² G. H. Briggs, Proc. Roy. Soc. (London) A114, 313 (1927).

* This work was supported in part by the U. S. Atomic Energy Commission with funds provided under contract AT(30-1)-3223, and by the National Science Foundation under Grant No. NSF G-23145.

† Present address: University of Florida, Gainesville, Florida.

¹ M. S. Livingston and H. Bethe, Rev. Mod. Phys. 9, 245 (1937).

² N. Bohr, Kgl. Danske Videnskab. Selskab, Mat. Fys. Medd. 18, No. 8 (1948).

³ H. A. Bethe and J. Ashkin, in *Experimental Nuclear Physics*, edited by E. Segrè (John Wiley & Sons, Inc., New York, 1952), Part II, Vol. I, p. 166.

⁴ U. Fano, Ann. Rev. Nucl. Sci. 13, 1 (1963).

⁵ L. C. Northcliffe, Ann. Rev. Nucl. Sci. 13, 67 (1963).

⁶ R. O. Bondelid and J. W. Butler, Phys. Rev. 130, 1078 (1963).

⁷ S. D. Warshaw, Phys. Rev. 76, 1759 (1949).

⁸ A. B. Chilton, J. N. Cooper, and J. C. Harris, Phys. Rev. 93, 413 (1954).

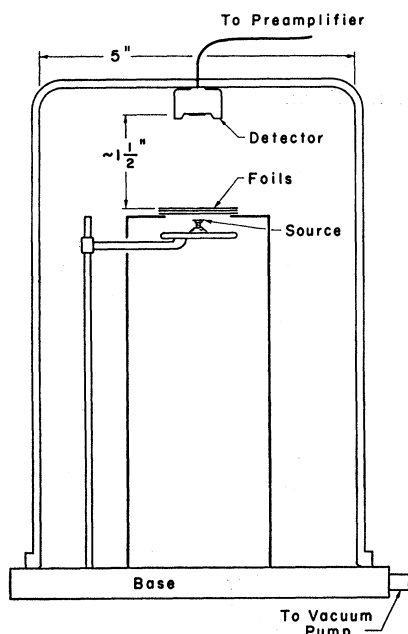


FIG. 1. Diagram of the experimental apparatus (not drawn to scale).

that all the thin foils used in this experiment had pinholes. Aluminum was especially bad in this respect. The other materials had very few pinholes. Nickel appeared to be the best. As will be explained below, it is believed that the experimental results provide internal evidence for assessing the uniformity of the foils. Except for aluminum, it is believed that the results to be reported are not severely limited by lack of uniformity.

B. Source and Apparatus

A Po^{212} source yielding a monoenergetic alpha-particle beam of energy 8.78 MeV was used in the present experiment. It was obtained from the decay sequence of thorium emanation (Rn^{220}) which had been coated on the head of a small thumb tack. The source also contained Bi^{212} which yielded alpha-particle groups at energies 6.086 and 6.047 MeV. These were used during calibration of the apparatus. Also used for calibration were the alpha-particle groups of energy 5.476 MeV from Am^{241} and energy 5.147 MeV from Pu^{239} .

A diagram of the apparatus is given in Fig. 1. The source was placed on a stage inside a cylindrical vacuum chamber. The latter was evacuated to approximately 80μ of Hg through a line containing a charcoal trap immersed in liquid air. The foils, now having been clamped into aluminum rings to maintain flatness, were placed on a second stage close above the source. No collimators were used, either between the source and foils or between foils and detector so as to avoid energy degradation resulting from slit-edge scattering.

A silicon surface-barrier solid-state detector with an active area of 25 mm^2 was used to detect the alpha par-

ticles which passed through the foils. It was placed approximately 4 cm above them. The energy loss resulting from the $50\text{--}100\text{-}\mu\text{g}/\text{cm}^2$ -thick gold surface was automatically corrected by the calibration. A depletion depth of 60μ obtained with 50-V bias was sufficient to stop all alpha particles with energies less than 10 MeV. The output from the detector was passed through a charge-sensitive preamplifier and then taken directly to the amplifier stage of a 400-channel pulse height analyzer.

C. Procedure

The energy calibration of the analyzer was obtained by using the four sources listed above. Although the Bi^{212} and Am^{241} sources each have two closely spaced alpha-particle groups and the Pu^{239} source has three such groups, it was found that the resolution obtained with the apparatus enabled one to obtain the location of the dominant group in each source with great accuracy. It was found that the region between 5 and 9 MeV could be very well represented by a straight line, the largest deviation between the energy of one of the sources and that obtained from the line being 8 keV. The rms deviation from all sources was 6 keV. Using a precision mercury-relay pulser, it was found that the electronics were also linear in the region corresponding to energies between zero and 5 MeV. The location of the 8.78-MeV group was periodically checked throughout the experiment and found to be stable to within two channels in 375.

The following procedure was used to measure the energy loss and straggling. With no foils on the stage, the chamber was evacuated and an energy spectrum of the Po^{212} alpha particles was taken. Then a single foil was placed on the stage and a new spectrum taken. The peak of the energy spectrum occurred in a lower channel and the distribution was broader. This foil was replaced with another foil and the process repeated until all foils of a given element had been examined singularly. Then two foils were placed in the chamber, one on top of the other, and a new spectrum taken. With the addition of more foils the peak of the energy distribution could be moved towards channel zero and large widths could be obtained. Counting was made for a time sufficient for the distributions to have a maximum count of about 500 per channel. Owing to the short half-life of the Po^{212} source material, a new source was provided every few hours.

III. RESULTS

A. Peak Widths and Peak Shapes

The output from the analyzer after each experimental run was plotted in the region around each peak. A smooth curve, estimated by eye, was drawn through the data points. In Fig. 2 the data for silver are shown, all superimposed on a single graph and normalized to the same maximum height. The increase in the widths of the peaks as the number of foils is increased is clearly seen.

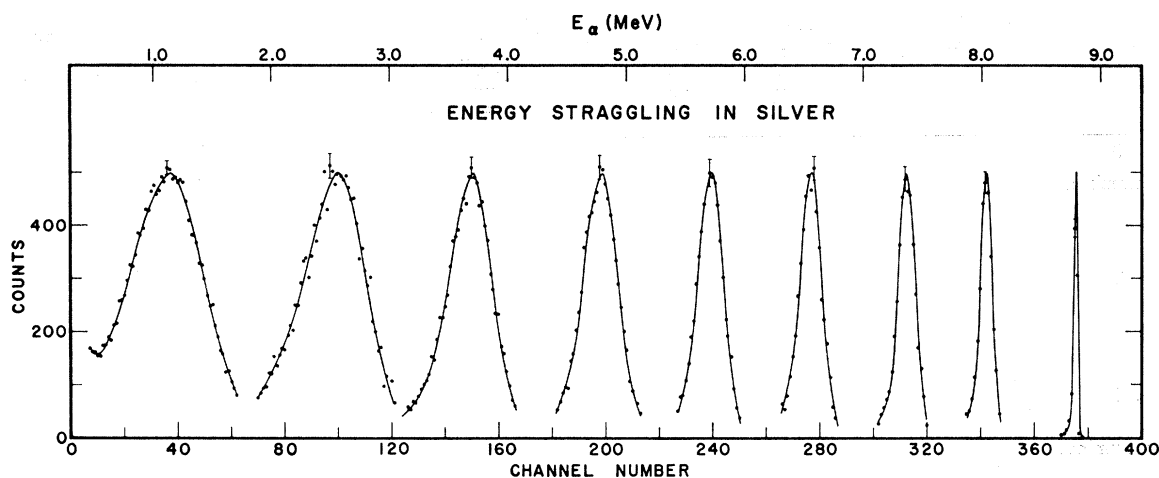


Fig. 2. The observed energy distributions of alpha particles straggling in silver. Increasing the number of foils degrades the energy and broadens the distribution. The solid curves are estimated by eye and normalized to 500 counts maximum.

The widths of the energy distribution arise from the energy-loss processes in the foils and from instrumental effects. Knowledge of the latter can be obtained from the calibration data taken with several sources without foils. The distribution seen with the Po^{212} source is plotted near channel 375 in Fig. 2. The full width at half-maximum (FWHM) for each Po^{212} source used was approximately 30 keV. It arises from the statistics of the electron-hole production processes in the detector, the straggling in the gold surface layer, and noise in the electronic circuitry. The width will add quadratically with the widths arising from straggling to yield the observed width. That is, if η is the FWHM resulting from straggling, then

$$\eta^2 = (\eta_{\text{total}})^2 - (\eta_{\text{inst}})^2.$$

In using the above subtraction it is important to know whether η_{inst} is significantly dependent on particle energies. By considering the statistical variation in the number of electron-hole pairs formed by the alpha particles in the detector, one can estimate that the FWHM resulting from this is approximately 6 keV at 8-MeV particle energy and 20 keV at 1 MeV. When subtracted in quadrature from peaks that are several hundred kilovolts wide, however, the increase from 6 to 20 keV is not significant and may be neglected. Similarly, straggling of alpha particles in the gold surface layer of the detector can enhance the corrected widths, if there is any energy dependence of the straggling. Using the results from this experiment, it is estimated that the FWHM resulting from straggling in a $100\text{-}\mu\text{g}/\text{cm}^2$ gold layer is approximately 6 keV at 8-MeV particle energy and could increase to 15–20 keV at 1 MeV. Again, when subtracted in quadrature, the increase is insignificant. Some information about the possible increase in linewidth with decreasing particle energy can be provided from the calibration spectra of the sources. Except for the Po^{212} source the widths were all equal to about 36 keV. However, as all these spectra

are composites of several alpha-particle groups, it was concluded that there was no significant change in linewidth from that of the Po^{212} source and that the 30-keV width may be assumed to be constant over the region between 5 and 9 MeV. Any increase at lower energies is believed to be negligible.

Also observed in Fig. 2 is the existence of low energy tails and consequent lack of symmetry in the distributions. Part of this arises from the response of solid-state detectors.¹³ Asymmetry has been predicted by Landau¹⁴ for fast particles traversing thin layers of material. An extension of this work by Promeranchuk¹⁵ and Orlov¹⁶ for very heavy particles and thick layers of material showed that Gaussian distributions should be expected. A detailed discussion of the problem has been given by Bohr,² who argued that, for heavy particles passing through thick layers of material, the energy distribution should be Gaussian with an additional low-energy tail being produced by a small number of violent collisions with nuclei. He argued further that the position of the maximum of the Gaussian portion of the distribution is very near the position of the maximum (the most probable value) of the experimental distribution and that its half-width at half-maximum (HWHM) nearly equals the HWHM of the experimental distribution measured on the high energy side. Since the conditions for Bohr's conclusions are met in this experiment and since all theoretical expressions for energy straggling assume Gaussian distributions, it has been decided that the best measure of the energy of the alpha particles emerging from a material is at the position of the maximum of the distribution and that the best measure of the straggling is the HWHM on the high-energy side. With very few exceptions, the results obtained if the

¹³ A. Chetham-Strode, J. R. Tarrant, and R. J. Silva, IRE Trans. Nucl. Sci. NS8, 59 (1961).

¹⁴ L. Landau, J. Phys. (USSR) 8, 201 (1941).

¹⁵ I. Pomeranchuk, Zh. Eksperim. i Teor. Fiz. 18, 759 (1948).

¹⁶ Iu. F. Orlov, Zh. Eksperim. i Teor. Fiz. 30, 613 (1956) [English transl.: Soviet Phys.—JETP 3, 647 (1956)].

TABLE I. Energy loss and straggling data.

No. of foils	Total thickness (mg/cm ²)	Energy (MeV)	Entire FWHM (keV)	Symmetric FWHM (keV)
0	0.0	8.78	30	30
Thin aluminum				
1	1.13	8.29	131	128
2	2.26	7.76	215	202
3	3.39	7.19	275	270
4	4.54	6.66	335	324
5	5.68	6.07	386	380
6	6.82	5.43	484	471
7	7.97	4.74	575	552
8	9.10	3.97	655	632
9	10.23	3.11	810	790
10	11.37	2.08	1030	995
11	12.50	0.84	>1360	1355
Thick aluminum				
1	4.16	6.72	170	160
2	8.32	4.19	283	278
3	9.48	3.35	418	410
4	10.61	2.38	588	575
Thin nickel				
1	1.45	8.28	64	57
1	2.21	8.04	84	82
2	2.55	7.90	86	81
3	4.05	7.37	112	100
4	5.65	6.75	140	119
5	6.95	6.25	160	151
6	9.35	5.21	220	197
7	11.72	4.05	251	241
8	13.93	2.84	360	324
9	16.26	1.18	541	496
Thick nickel				
2	8.97	5.42	233	224
3	13.46	3.20	372	360
Silver				
1	2.90	8.02	110	110
2	5.62	7.36	170	160
3	8.28	6.54	220	215
4	11.18	5.70	251	242
5	13.86	4.77	354	342
6	16.73	3.68	437	406
7	19.55	2.56	620	565
8	22.31	1.13	761	686
Gold				
1	4.30	8.03	142	123
2	8.75	7.06	270	252
3	13.23	6.15	370	286
4	17.78	5.17	467	390
5	22.12	4.05	579	534
6	26.28	2.98	700	588
7	30.73	1.59	1015	814

entire asymmetric FWHM's were used lie within the errors assigned to the results calculated from the symmetric FWHM's, the deviations slowly increasing with increasing foil thickness.

The basic results of this experiment are given in Table I. Listed for each element are the total foil thicknesses, the most probable energies of the alpha particles after emerging from the material, and the asymmetric and symmetric FWHM's. Results obtained from thick aluminum and nickel foils are listed separately. A conservative estimate of errors was used in the subsequent analysis. It was judged that the position of the maximum of each distribution can be determined with a precision less than 10% of the FWHM. A value

TABLE II. The most probable projected ranges of 8.78-MeV alpha particles are compared with recent values of Whaling. Whaling's value for Ni is apparently the result of an error in the tables and a value near 19.0 mg/cm² is more probably correct.

Material	This experiment (mg/cm ²)	Whaling (mg/cm ²)
Al	13.0	14.4
Ni	17.4	20.0
Ag	23.7	25.5
Au	34.3	35.6

of 8% was used. Hence the FWHM is believed known to 15% of its value.

B. Energy-Thickness Relations

The data from the second and third columns of Table I may be plotted to yield curves of the energy of alpha particles which have passed through foils of various thickness R . The graphs are shown in Fig. 3. The excellent agreement between the results for the thin and thick Ni foils is to be noted. The discrepancy in the corresponding results for Al cannot be explained by the errors in E or R . It is suggested, however, that if the thin foils are nearly uniform except near pinholes, then the observed energy distributions will be broadened to the high-energy side and thus the values of E plotted on the graph will be too high.

By drawing a smooth curve through the data points and extrapolating to zero energy, values of the most probable projected range R_{\max} will be obtained. Because of the slight asymmetry of the energy distributions, the mean projected range may be slightly less. The transformation of coordinates ($R \rightarrow R_{\max} - R$, $E \rightarrow E$) will yield the customary range-energy curves. Values of R_{\max} obtained by extrapolation are listed in Table II and compared with the calculated values of Whaling.¹⁷ The fact that the experimental projected ranges are less than the calculated values is in agreement with expectations since the latter represent the total path-length in the material and multiple scattering corrections have not been applied.

C. Stopping Powers

The stopping powers $-dE/dX$ may be approximated by the quantity $-\Delta E/\Delta X$, where ΔE is the average energy loss in a foil of thickness ΔX . This quantity is normally plotted against the average energy in the foil $E_{\text{av}} = (E_i + E_f)/2$, where E_i and E_f are the initial and final average energies. The approximation is valid if ΔE is small compared to E_{av} . Chilton *et al.*⁸ argue that if the approximation is used, then the stopping power could be plotted against an energy E' differing from E_{av} by a small amount. Using the expression derived by these authors it was found that the maximum correction to the E_{av} in the present data is less than 1.5%. The corrections have been subsequently neglected.

The stopping powers $-dE/\rho dx$ have been plotted in ¹⁷ W. Whaling, in *Encyclopedia of Physics*, edited by S. Flugge (Springer-Verlag, Berlin, 1958), Vol. 34(1), p. 193.

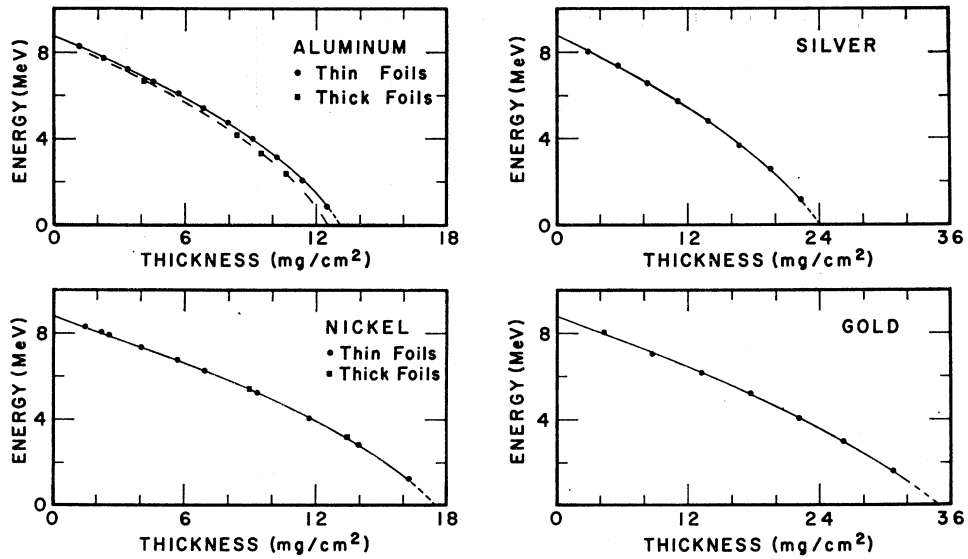


FIG. 3. The most probable energy of each observed distribution is plotted against the total material thickness. The discrepancy for Al is not fully explained. Curves are estimated by eye.

Fig. 4 as a function of E_{av} . The density ρ is included in the denominator. Also shown in the figure are curves of Bichsel¹⁸ calculated from the Bethe¹⁹ theory. They were calculated from the expression

$$-\frac{1}{\rho} \frac{dE}{dx}(E) \Big|_{\alpha} = -\frac{1}{\rho} \frac{dE}{dx} \left(\frac{E}{4} \right) \Big|_p z^{*2}, \quad (1)$$

where z^* is the effective charge of the alpha particles in the foils (to be discussed more fully below) and $-dE/\rho dx$ is tabulated for protons by Bichsel with a quoted accuracy of 2–10%. There is very good agreement between the theoretical and experimental values except for Ni, where the experimental values are systematically high. The discrepancy is consistent with the fact that the observed R_{max} for Ni is much less than the calculated value.

D. Straggling

The data from Table I may be used to express the energy straggling of the alpha particles as a function of material thickness and of energy. In the former case the data from columns 2 and 5 may be plotted directly and will show the increase in the energy spread of an initially monoenergetic beam of particles as it passes through an increasingly thick layer of material. This is done in Fig. 5 along with the results of theoretical calculations (Sec. IV). The most interesting feature of the data is the occurrence of a rise in the experimental values at large thicknesses which is not predicted by the theories.

The second manner of considering the data is to calculate in quadrature the increase in straggling width with each successive addition of a foil. By subtracting out the effects of all the previous foils, the straggling in the last foil may be plotted as a function of average

alpha-particle energy in that foil. Because the foils for a given material do not all have the same thickness, the results have been normalized to unit thickness by defining a new parameter η_n' for the n th foil of thickness ΔX_n such that

$$\eta_n'^2 = [\eta_n^2 - (\eta_{n-1})^2] / \Delta X_n. \quad (2)$$

where η_n is the FWHM resulting from n foils. The results are shown in Fig. 6, also with theoretical predictions. A rise in the experimental values at low energies is again clearly seen. This will be discussed later.

IV. THEORETICAL CALCULATIONS

Three theories describing the energy-loss processes of charged particles in matter which have achieved

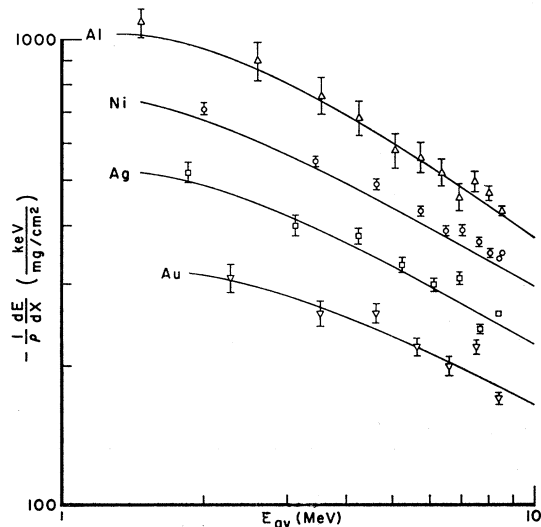


FIG. 4. Stopping powers for alpha particles as a function of particle energy. The curves are theoretical, obtained from tables of Bichsel.

¹⁸ H. Bichsel, in *American Institute of Physics Handbook* (McGraw-Hill Book Company, New York, 1963), 2nd ed., Sec. 8c.

¹⁹ H. Bethe, *Ann. Physik* 5, 325 (1930).

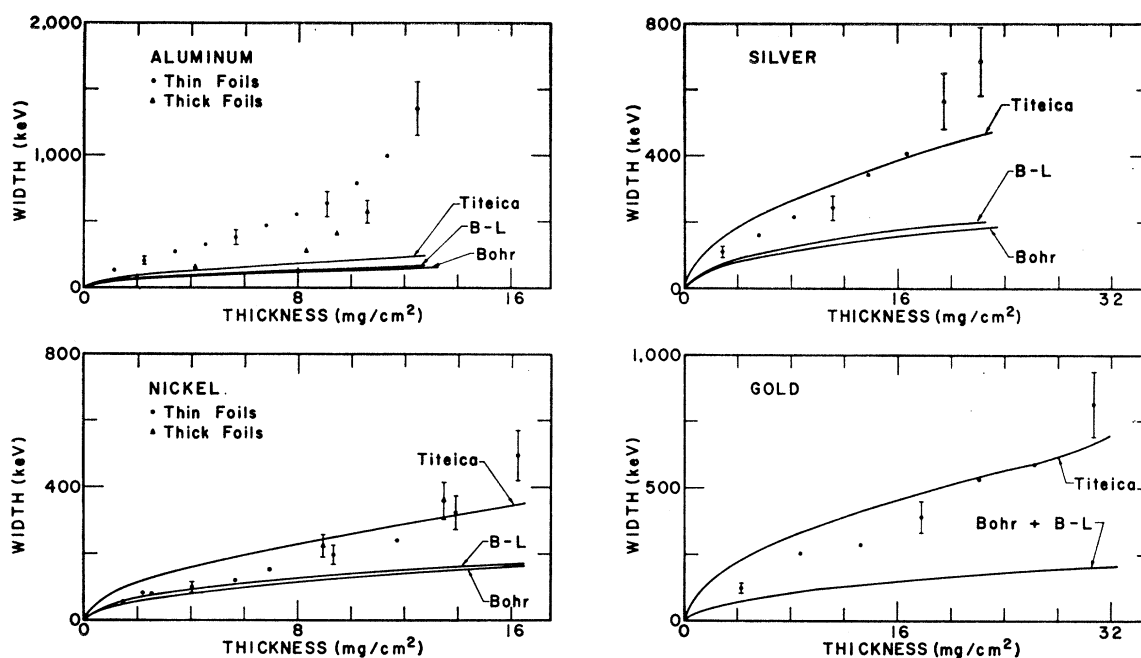


FIG. 5. Symmetric FWHM's η are plotted against material thickness along with theoretical curves. The Bohr and Bethe-Livingston curves cannot be distinguished for gold.

general notice have been the classical-mechanical theory of Bohr,^{20,2} and the quantum-mechanical theories of Bethe¹⁹ and Bloch.^{21,22} Associated with each of these is an expression for straggling: the Bohr,²³ Bethe-Livingston,¹ and Titeica²⁴ formulas, respectively. The region of validity is not the same for each expression, as is discussed in detail by Northcliffe.⁵ In all cases it is assumed that the velocity of the ion is much greater than the orbital velocities of the atomic electrons. This assumption is poorly met in the present experiment. In addition, if one defines the parameter $\kappa = 2ze^2/\hbar v$, where ze is the charge of the incident ion

which has a velocity v , then, in general, the Bohr theory is valid for the region $\kappa > 1$, the Bethe theory is valid for $\kappa < 1$, and the Bloch-Titeica theory is valid for all values of κ . Hence the Bohr and Bethe theories are complementary. The critical alpha-particle energy for which $\kappa = 1$ is about 1.6 MeV. Hence the present experiment is investigating a region of overlap between two theories. Consequently, values of straggling will be calculated in turn from all three expressions.

A. Bohr Formula

The simplest of the three straggling expressions is that of Bohr.²³ The standard deviation of a Gaussian distribution of energies is given as

$$\Omega^2 = 4\pi z^2 e^4 N Z (\Delta X), \quad (3)$$

where ze is the charge on an ion passing through a layer of material of thickness ΔX and containing N atoms per cm^3 having an atomic number Z . Values of η and η' , related to the standard deviation Ω by the relation $\eta = 2(2 \ln 2)^{1/2} \Omega$, have been calculated and are drawn in Figs. 5 and 6.

The Bohr expression depends only on the constitution of the medium and its thickness. It is not a function of the energy of the ions. Hence the curves in Fig. 5 should be parabolic and those in Fig. 6 should be horizontal lines. However, inclusion of an effective charge z^* will modify the results slightly at low energies. Corrections for effective charge have been included in this and all subsequent calculations. Values were taken from Evans²⁵ at values of v corresponding to $E_{\alpha v}$ in each foil.

²⁵ R. D. Evans, *The Atomic Nucleus* (McGraw-Hill Book Company, Inc., New York, 1955), p. 636.

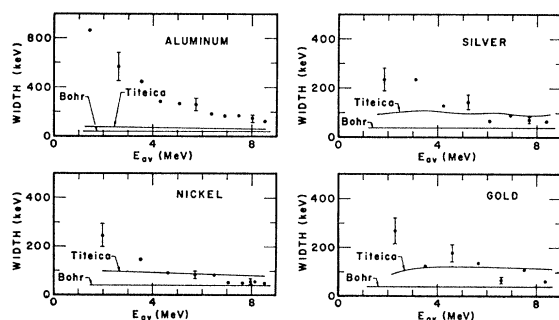


FIG. 6. Straggling widths η for individual foils are plotted against the mean alpha-particle energy in the foils and compared with theoretical curves. The wiggles in the Titeica curve for Ag arise from the method of calculation and are not believed to be significant.

²⁰ N. Bohr, *Phil. Mag.* **25**, 10 (1913).

²¹ F. Bloch, *Ann. Physik* (5) **16**, 285 (1933).

²² F. Bloch, *Z. Physik*, **81**, 363 (1933).

²³ N. Bohr, *Phil. Mag.* **30**, 581 (1915).

²⁴ S. Titeica, *Bull. Soc. Roumaine Phys.* **38**, 81 (1939).

B. Bethe-Livingston Formula

From the treatment of Livingston and Bethe¹ it is found that the straggling is measured by the standard deviation

$$\Omega^2 = 4\pi z^2 e^4 N \left[Z' + \sum_i k_i \frac{I_i Z_i}{mv^2} \ln \frac{2mv^2}{I_i} \right] (\Delta X). \quad (4)$$

In addition to the definitions given after Eq. (3), m is the mass of the electron, v is the velocity of the incident ion, Z' is the total number of effective electrons, I_i is the average excitation energy of the Z_i electrons in the i th atomic orbit, and k_i is a constant taken to be 4/3 for all orbits. The summation extends over all orbits for which $2mv^2 > I_i$. Hence the Bethe formula is similar to that of Bohr, except for the reduction in the charge Z' and the inclusion of terms depending on atomic structure. As a result of the v^2 factors, there is a slight energy dependence of Ω^2 . The evaluation of Eq. (4) raises several problems which shall be considered separately.

(a) Evaluation of I_i

A set of average excitation energies must be found which satisfies the general relationship given by Bethe¹⁹

$$Z \ln I = \sum_i f_i \ln I_i, \quad (5)$$

where I is the average ionization potential of the atom of charge Z and f_i is the sum of the oscillator strengths for all transitions of an electron of the i th orbit. This equation may be taken as the definition of I . The values of f_i are approximately equal to Z_i and must satisfy the condition $\sum_i f_i = Z$. In first order the excitation energies I_i may be taken to be the observed x-ray critical absorption energies $h\nu_i$. In general, however, these will not satisfy the sum rule.

The evaluation of a set of energies I_i has been done with the aid of a recipe given by Sternheimer.²⁶ The sum rule, Eq. (5), is rewritten as

$$\sum_{i=1}^{j-1} f_i \ln I_i + f_j \ln (h\nu_j f_j^{1/2}) = Z \ln I, \quad (6)$$

where the summation extends over all orbits except the j orbit, which contains conduction electrons. The plasma frequency is $\nu_p = (NZe^2/\pi m)^{1/2}$. The energy I_i is then replaced by $\rho h\nu_i$, where $h\nu_i$ is the x-ray critical absorption energy for the i th orbit and ρ is a correction factor applied to all $h\nu_i$. The factor ρ must then be evaluated.

Values of $h\nu_i$ have been tabulated by Landolt-Börnstein²⁷ for orbits specified by the quantum numbers n , l , and j . Values of I have been taken from the recent tabulation of Fano⁴ and f_i has been set equal to Z_i . Values of ρ have been calculated from Eq. (6). They varied in a range from 2 to 3.2. Hence values of $I_i = \rho h\nu_i$

²⁶ R. M. Sternheimer, Phys. Rev. 88, 851 (1952); 103, 511 (1956); and 117, 485 (1960).

²⁷ H. H. Landolt-Börnstein, *Zahlenwerte und Funktionen*, (Springer-Verlag, Berlin, 1950), 6th ed., Vol. I, Part 1, pp. 226-228.

are obtained for the core electrons. Values of I_i for the conduction electrons were obtained from the NBS atomic energy level tables.²⁸ As a final check on the calculations, the set of I_i thus obtained was substituted into Bethe's sum rule. The agreement between the two sides of the equation was always good.

(b) Evaluation of Z'

Sternheimer²⁶ took Z' to be the sum of all electrons in orbits not excluded in Eq. (4) by the condition $I_i > 2mv^2$, i.e., $Z' = \sum_i Z_i$. Livingston and Bethe,¹ however, note that such a value is incorrect and write instead $Z' = Z - \sum_j f_j Z_j$, where now the sum extends over the electrons excluded in Eq. (4) by $I_i > 2mv^2$. The f_j is an oscillator strength for the optical transitions into the continuous spectrum and differ from unity. Values of f_j have been calculated by Hönl²⁹ for the K and L electronic orbits. These are sufficient for Al and Ni, but values for M and N orbits are also needed for Ag and Au. They have not been calculated, but are not expected to differ appreciably from unity. Since the results for Ω^2 obtained with the Hönl values for the K and L orbits are nearly identical to those obtained using the Sternheimer approximation, the neglect of the corrections for the M and N shells is not believed to be important.

(c) Energy Dependence

Because v^2 in Eq. (4) decreases as ΔX increases, energy thickness curves, such as those in Fig. 2, must be included in the evaluation of Eq. (4). This has been done using the data listed in Table I. Using $v^2 = 2E_{av}/M\alpha$, Ω_i^2 is calculated for each foil separately. Then the total Ω^2 for n foils is $\Omega^2 = \sum_i^n \Omega_i^2$. The use of a constant v^2 in each foil is questionable. Yet a check was available since Ω^2 could be calculated for both thin foils and thick foils of Al and Ni. The agreement was exact.

Equation (4) has been evaluated for the four elements and the results for η are shown in Fig. 5. Effective charges were included. The curves lie slightly above those of the Bohr formula. The energy dependence, as calculated by Eq. (2), could not be distinguished from that of the Bohr formula and so was not plotted in Fig. 6.

C. Titeica Formula

Applying the method of Bloch, Titeica²⁴ found that he could express the straggling width as

$$\Omega^2 = 4\pi z^2 e^4 N Z \left\{ 1 + \frac{4 E_{kin}}{3 mv^2} \times \left[\ln \frac{2mv^2}{I} + \psi(1) - \text{Re} \psi \left(1 + i \frac{ze^2}{h\nu} \right) \right] \right\}. \quad (7)$$

²⁸ *Atomic Energy Levels*, edited by C. E. Moore, Natl. Bur. Std. Circ. No. 467, (U. S. Government Publishing and Printing Office, Washington, D. C., 1949, 1952, and 1958), Vols. I-III.

²⁹ H. Hönl, Z. Physik 84, 1 (1933).

In addition to the meanings already assigned to the symbols, E_{kin} is the average kinetic energy per electron of the electrons in the stopping material, ψ is the logarithmic derivative of the gamma function, and $\text{Re } \psi$ is the real part of ψ . Equation (7) has an appearance very similar to Eqs. (3) and (4). It will, in fact, reduce to the Bohr formula when $ze^2/hv \gg 1$ and to the Bethe-Livingston formula when $ze^2/hv \ll 1$.

In the evaluation of (7), I is again taken from the tables of Fano.⁴ E_{kin} has been evaluated by Hund³⁰ from a Thomas-Fermi model of the atom. An expression

$$E_{\text{kin}} = 20.8 Z^{4/3} \text{ eV} \quad (8)$$

is obtained. Calculations of Eq. (7) have been carried out using effective charges and including the energy dependence in the same manner as in the Bethe-Livingston formula. The results are plotted in Fig. 5. The widths η are 2-3 times greater than those of the previous calculations, a difference arising primarily from the E_{kin} factor. The shapes are not substantially different. The energy dependence, calculated from Eq. (2), is plotted in Fig. 6.

V. CONCLUSIONS

The most obvious features of the straggling data are that they are not very well represented by any of the theoretical curves and that the deviation is enhanced at low particle energies. In general, the data lie between the curves of the Bohr and Titeica formulas except in the case of low energies and for aluminum at all energies, where it rises above both of them. The data approach the Bohr curves at small foil thicknesses.

Some explanation for the discrepancies can be provided by the lack of uniformity of the foils. The aluminum foils are known to have numerous pinholes and the radical behavior of the data for that element is evidence of the fact. It is important to note that the discrepancy was greatly reduced by using the more uniform thick Al foils. The nickel foils are believed to be the most uniform and the data are, in fact, in closest agreement with the Bohr curve. The agreement between the data for thin and thick nickel foils is strong evidence for their uniformity. The similarity of the silver and gold data to the nickel data is taken as evidence for the relative homogeneity of those foils.

It is unlikely that foil inhomogeneities could account for the large rises in the straggling observed at low energies. A possible explanation for these could be a large increase in path length as a result of multiple scattering. This effect is difficult to calculate. Rough estimates have been carried out using the tables of Bichsel.¹⁸ Particles emerging from a layer of material have an angular distribution from the normal which is roughly Gaussian in shape, with a standard deviation

half-angle less than 3° for low Z or high energy and as much as 10° for low-energy particles in high- Z material. From the geometry of the apparatus, considering the source as a point, it is estimated that the half-angle acceptance of the detector is less than 5° . Hence it is more probable that the particles which are detected are those which have undergone few scatterings and have not had a great increase in path length. It may also be argued that the technique of comparing only the symmetric FWHM of each distribution against theory has the effect of neglecting those particles which have lost considerable energy as a result of a large increase in path length from multiple scattering. Nevertheless, detailed calculations of multiple scattering at very low energies are needed.

An alternative explanation for the observed low-energy behavior lies in the behavior of the charge of the alpha particles. An effective charge $z^* < z$ arises from fact that not all ions have a charge $z=2$, but that some have a charge $z=1$. The calculation of stopping powers and ranges can be made quite successfully with a velocity-dependent z^* . But it is not strictly valid to equate z with z^* in the straggling formulas. Effective charges were included in Sec. IV to show that their effect was opposite to the observed behavior. Physically, ions with charge $z=1$ will not lose energy as rapidly as ions with charge $z=2$ and hence, on emerging from a foil, will have an average energy larger than those of charge two. As a result of fluctuations in the charge exchange processes, the resulting energy distribution will not separate into two groups but will more probably be broadened. For alpha particles, capture and loss of electrons begins to become significant in the energy region below 4 or 5 MeV. The data in Fig. 6 are consistent with this interpretation. Calculations of this effect, however, are beyond the scope of this report.

The foils used in this experiment are typical of those used by many experimental physicists. Because of its great simplicity, it is suggested that, for practical applications, the straggling of alpha particles be calculated with the Bohr equation. The result should be then multiplied by a factor between 1 and 2, the amount depending on the alpha-particle energy and the material thickness. Estimates of the factor may be obtained from the data presented here. For small thicknesses or large energies, the Bohr formula gives good results. However values are too small for large thicknesses or low energies by a factor of 2 or more.

ACKNOWLEDGMENTS

The authors are pleased to acknowledge the Technical Measurements Corporation for lending them a model 402 pulse-height analyzer. Thanks are due to Professor L. C. Northcliffe for his interest, encouragement, and assistance. Special thanks are extended to Dr. J. E. E. Baglin for his interest, and for carefully reading the manuscript.

³⁰ F. Hund, in *Handbuch der Physik*, edited by H. Geiger and K. Scheel (Springer-Verlag, Berlin, 1933), 2nd ed., Vol. XXIV(1), p. 622.